

## Modelling and Simulation of a Grid-Connected PV System based on Efficient Maximum Power Point Tracking Algorithm

F. Q. Al-Enezi, M. Rotaru, J. K. Sykulski

Electronics and Computer Science, Faculty of Physical Sciences and Engineering, University of Southampton, UK

### Abstract—

The results presented in this paper have been acquired through simulation of a grid-connected photovoltaic system (GCPV) to a specific section of Alsabyia generation station part of Kuwait national grid with efficient maximum power point tracking (MPPT) algorithm incorporated into a DC-DC boost converter. The simulations were performed using Power Simulation Software (PSIM). The analytical model of a photovoltaic (PV) module has been combined with a ‘perturb and observe’ (P&O) method so that MPP is achieved with the external temperature and solar radiation (SR) also considered. A DC-AC inverter is used to track the output voltage of the converter and interface the PV array with the grid. The results show that the model not only achieves the MPP function but also improves the output of the inverter by reducing the ripples in the sine waveforms.

**Index Terms—** Solar radiation (SR), Grid-connected photovoltaic (GCPV), Maximum power point tracking (MPPT)

### I. INTRODUCTION

When larger PV installations are designed, there is a need to understand their performance when integrated with the power system (a specific section of Alsabyia generation station part of Kuwait national grid). Therefore, simulations of large PV installations integrated within the electrical grid are necessary. Numerically the problem that needs to be solved is a combination of non-linear equations describing the PV generators, including the switching inverters, operational DC-DC converter and the PV generation with linear equations describing the rest of the power system. Many studies have discussed and proposed solutions to the numerical problems posed by GCPV power simulations [1, 2]. From a purely mathematical point of view, at each step of the simulation, the set composed of non-linear equations representing PV generators and linear equations describing the rest of the power system must be solved, using an iterative numerical algorithm [2]. Some power system simulation tools adopt this approach, such as PSIM and MATLAB/Simulink. This approach is accurate, but with the drawback of a heavy computational burden when simulating large distribution networks including PV systems [3]. Moreover, the non-linear equations introduce a dependency of the current injected by a PV generator on the terminal voltage, which in turn is related to the operating conditions of the whole power system. Such a dependency can cause numerical instability of the simulation [4].

### II. GCPV SYSTEM SIMULATION SETUP

The system considered in this study consists of a PV module, a DC-DC boost converter and a DC-AC

inverter. The system described here uses a simplified PV cell model however, the model includes the effects of changing the SR. The maximum power of the PV module is tracked with the help of an MPPT algorithm that is incorporated into the DC-DC converter. The inverter used to regulate the output voltage of the converter is connected to the rest of Alsabyia grid through an LC filter which ensures clean current injection.

Figure 1 shows a general topology of a PV generation system. The PV depicted below is a standard integrated PV system connected to a DC-DC converter and then to a pulse-width modulated (PWM) DC-AC inverter. Since the output voltage of the PV module has a very broad voltage range, in general a DC-DC converter is used to ensure constant high output DC voltage with MPPT to track the maximum power of the PV system. In order to use the DC output power for residence applications, it is required to convert the DC output power to AC power using a PWM inverter.

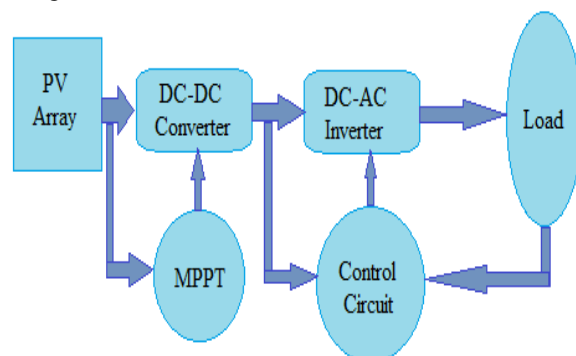


Figure 1: Schematic diagram of a complete PV generation system

The simulation process is quite sophisticated. It uses a current-voltage ( $I$ - $V$ ) curve characterization of the PV module accounting for the instantaneous cell temperature. We chose to evaluate a specific area in a square meter off-grid PV array in Kuwait not far away from Alsabyia grid. Specifications (input variables for the simulation process) carried in the database and transferred to the PV simulation are:

- Total SR over Kuwait area.
- Actual capacity of the PV array.
- Length and width of the PV module.
- Open-circuit voltage.
- Short-circuit current.
- Voltage temperature coefficient.
- Current temperature coefficient.
- Number of modules in series.
- Number of modules in parallel.
- Panel configuration.
- Characteristics of the selected PV module: efficiency, cell temperature, sizing factor and temperature coefficients.
- Characteristics of the selected inverter: AC power, voltage, PV voltage range at maximum power, maximum efficiency and maximum input current.

The system characteristics are system voltage, current, panel capacity, mismatch, and the inverter power and inverter efficiency at rated power. In the algorithm presented here, which simulates the GCPV system, the controller is assumed to achieve cell operation at the MPP. In the following sections of the paper each of the important parts of the model will be introduced and explained. First the PV cell model is introduced. The model is simple, accurate, and takes SR into consideration. Then the MPPT control algorithm is discussed. The P&O method is then used in conjunction with the MPPT algorithm. The results obtained from a PSIM simulation are also presented. Section III explains the reasons for using a boost converter for this application as a DC-DC converter, and it discusses the operating principles. Finally, the last part of the system, the DC-AC inverter, is discussed before the whole PV system is presented. The system simulation results are presented and discussed.

### III. SYSTEM COMPONENTS

Simulation of the system is not an end in itself; it is to permit insight into the operation of the system in such a way that weaknesses can be identified. The proposed model of the entire components and control system are all simulated in PSIM Software. The simulation results under PSIM show the control

performance and dynamic behavior of the GCPV system.

#### 1) PV Module

The single-diode equivalent circuit is the most commonly adopted model of PV cells, accounting for the photon-generated current and the physics of the  $p$ - $n$  junction of a PV cell. The simulation structure of the PV model in PSIM has been shown in Figure 2.

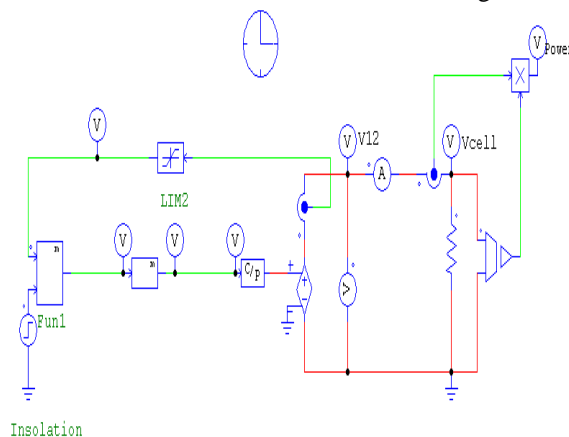


Figure 2: Simulation structure of PV model

A PSIM program was used to validate the developed solar module model. The parameters used to define the PV cell are shown in Table 1.

Table 1: Parameters of the PV Cell in PSIM Model

Parameter	Variable	Value
Current at Maximum Power	$I_m$	4.95 A
Voltage at Maximum Power	$V_m$	35.2 V
Open Circuit Voltage	$V_{oc}$	44.2 V
Short Circuit Current	$I_{sc}$	5.2 A
Temperature Coefficient of Short Circuit Current	$a$	0.015 A/ $^{\circ}$ K
Temperature Coefficient of Open Circuit Voltage	$b$	0.7V/ $^{\circ}$ K
Internal Series Resistance	$R_s$	0.217 $\Omega$
Reference Solar Radiation	$SR_{ref}$	1000 W/m <sup>2</sup>
Reference Temperature	$T_{ref}$	25 $^{\circ}$ C

The PV-side DC voltages, currents and power are illustrated in Figures 3 to 5. As expected, the results obtained with this simulation show that the PV module voltage, current and power settle to 52 V, 5.7 A and 293 W, respectively, after a brief transient due to the switching. These results gave us confidence in the PV module model. The output is a voltage that

drives an assumed resistive load,  $R_L$ . Note that the solar panel current can be varied by changing the load resistance and both voltage and current at the output of the solar panel can be tracked and measured. It is encouraging that there is very good agreement between expected (53 V, 5.8 A) and simulated signals ( $E_{PV}$ ,  $I_{PV}$ ).

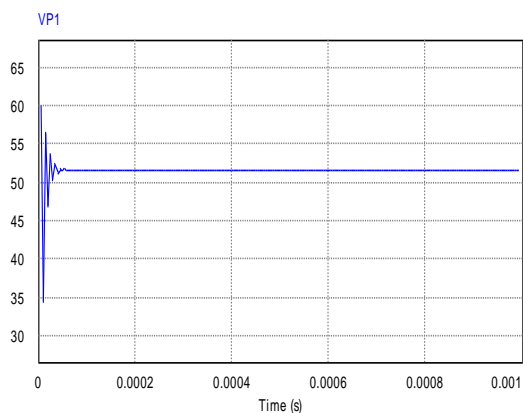


Figure 3: PV-side voltage waveform per module

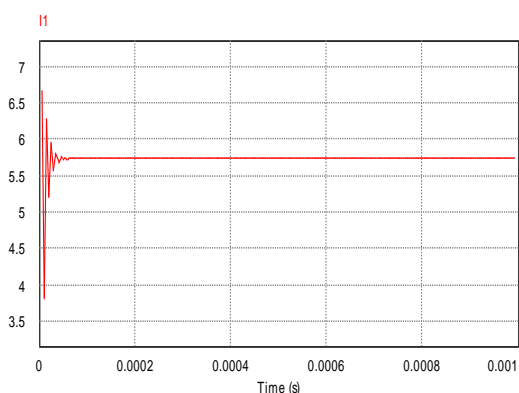


Figure 4: PV-side current waveform of per module

The simulation results for the  $I-V$  and  $P-V$  curves are shown in Figures 6 and 7. Figure 6 shows the  $I-V$  characteristic curve of one PV string, while Figure 7 shows the  $P-V$  characteristic curve. The model curves show three significant details: the short-circuit current, the open-circuit voltage, and the maximum power point. It can be noticed that the PV string behaves like a current source when the output voltage is less than a threshold value as the current changes very little with the change in output voltage whereas above the threshold voltage it behaves more like a voltage source with a sharp drop in current as the voltage is increased.

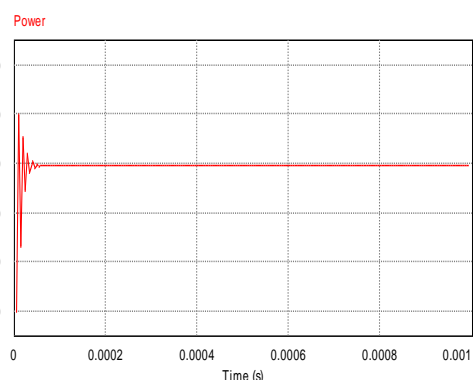


Figure 5: PV-side power waveform per module

The span of the  $I-V$  curve of one PV string ranges from the short circuit current ( $I_{SC} = 275$  A) at zero volts, to zero current at the open circuit voltage ( $V_{oc} = 3650$  V). At the ‘knee’ of a normal  $I-V$  curve there is a point where the PV cell generates the maximum power, called the maximum power point, MPP, ( $I_{mp} = 250$  A,  $V_{mp} = 3000$  V). In an operating PV system, one of the jobs of the inverter is to constantly adjust the load, seeking out the particular point on the  $I-V$  curve at which the array as a whole yields the greatest DC power. At voltages well below  $V_{mp}$ , the flow of solar-generated electrical charge to the external load is relatively independent of output voltage. Near the knee of the curve, this behavior starts to change. As the voltage increases further, an increasing percentage of the charges recombine within the solar cells rather than flowing out through the load. At  $V_{oc}$ , all of the charges recombine internally. The maximum power point (MPP =  $P_{max}(string) = 750$  kW), located at the knee of the curve, is the ( $I$ ,  $V$ ) point at which the product of current and voltage reaches its maximum value.

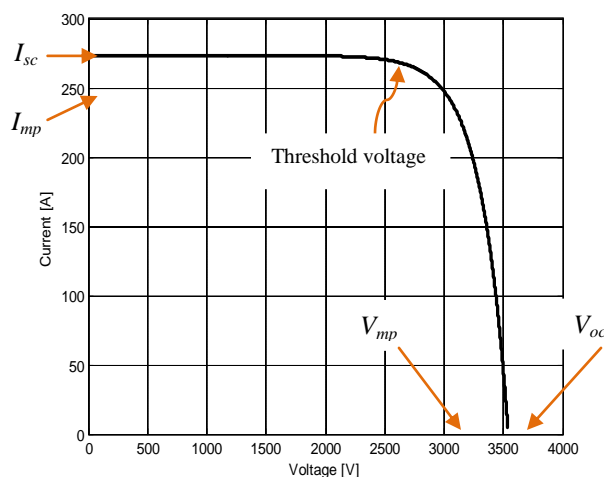


Figure 6:  $I-V$  characteristic of one PV string

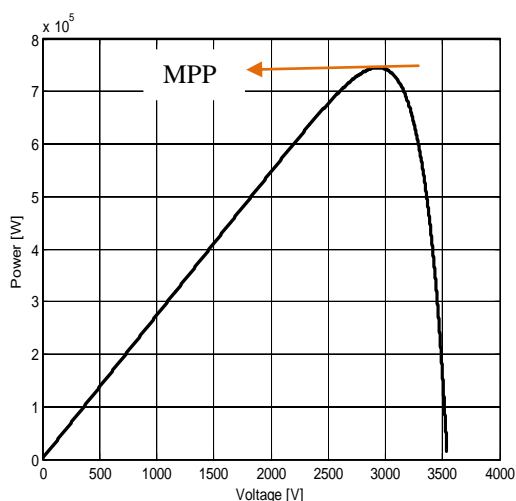


Figure 7: P-V characteristic of one PV string

## 2) Maximum Power Point Tracking (MPPT) Control Algorithm

An MPPT is used to extract the maximum power from the PV cell and transfer it to the load [5]. Since the output power of a PV cell is related to many parameters, such as SR, temperature and load, the output characteristic is nonlinear with respect to the output voltage. It is necessary for the PV system to work at the maximum power point under changing external environment to achieve best performance. Furthermore, this point depends on the SR and temperature of the panels and both conditions change during the day and are different depending on the season of the year. Moreover, SR can change rapidly due to changing atmospheric conditions such as clouds. It is very important to track the MPP accurately under all possible conditions so that the maximum available power is always obtained. Improving the tracking of the MPP with the developed control algorithms (see Figures 9 and 10) is easier, not expensive and can be done even in plants which are already in use by updating their control algorithms, which would lead to an immediate increase in PV power generation and consequently a reduction in its price [6]. On the other hand, trying to improve the efficiency of the PV panel and the inverter, although important, is not simple and could be very costly as it depends on many variables and manufacturing technologies available.

MPPT algorithms are necessary in PV applications because the MPP of a PV panel varies with the SR, so the use of MPPT algorithms is required in order to obtain the maximum power from a PV array. In this study, we chose the Perturb and Observe (P&O) method for its simplicity, relative accuracy and rapid response [7-8]. The P&O method involves a perturbation in the operating voltage of the DC link between the PV array and the power converter. This method is easy to implement, because

the sign of the last perturbation and the sign of the last increment in the power are used to decide what the next perturbation should be. If there is an increment in the power, the perturbation should be kept in the same direction and if the power decreases, then the next perturbation should be in the opposite direction. Using these observations, the algorithm is implemented. The process is repeated until the MPP is reached. Then the operating point oscillates around the MPP. Figure 8 shows the flowchart of the P&O method. By comparing the PV cell output power of each control cycle before and after the perturbation, the new perturbation direction can be determined. If the output power is increasing, the previous voltage perturbation direction will be followed in the new cycle. Otherwise, the voltage perturbation direction will change. By this algorithm, the operating point of PV cell can get closer to the maximum power point and finally reach a steady state.

One of the objectives of this study is to develop a model to test the dynamic performance of the MPPT algorithm shown in Figure 8 independently of the converter used. A detailed model of a PV system, with the switching model of the power converter, is computationally very demanding while the time that can be simulated in a normal computer is only a few seconds. However, the simulation time required for testing the system with the SR profiles can be up to several minutes, which can be difficult or impossible to achieve on conventional PC, if a complete model of the PV system would be used. The main limitation for such simulation is the limited amount of memory available on a conventional PC. For example, to increase the reference voltage and go back to compute the new output power the program has to check again all the power values with different average daily and monthly SR and this process takes several minutes.

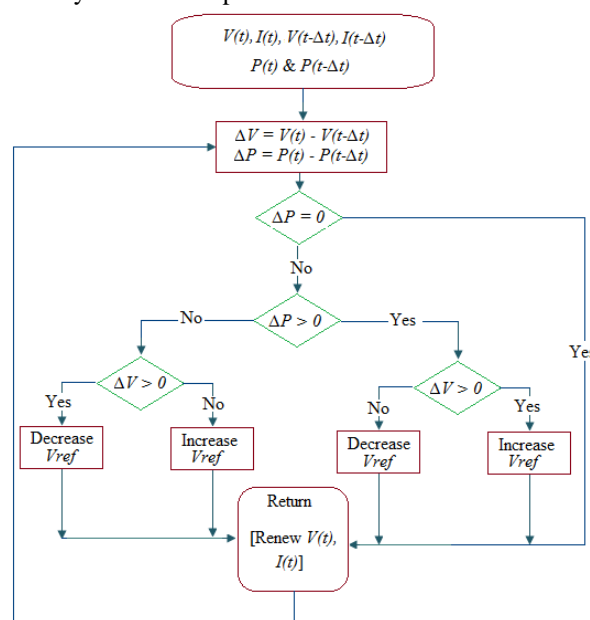


Figure 8: Flowchart of P&O method

The model proposed here was developed in PSIM and consists of a PV array model, a DC-link capacitor and a controlled current source, which replaces the power converter. The MPPT control block generates the reference voltage using the algorithm under test (see Figure 9a). The reference voltage generated by the MPPT control block is converted to a current reference using the control scheme shown in Figure 9b. In this scheme, the error between the reference and the actual DC voltage (the output voltage of the PV array) is fed in a proportional gain, whose value depends on the DC link capacitance and the sampling period. The output of this gain is subtracted from the current of the PV module and the result is the reference current for the controlled current source.

As the model is more complex, the simulation time can be much longer, the time needed to simulate 130 seconds is only a few minutes, and the simulation time can be over 1000 seconds. However, if the model includes a detailed switching power converter model, for example a three phase inverter, the simulation time can be only a few seconds and the time needed for MPPT efficiency tests is much longer.

The simulation model for the P&O MPPT algorithm is shown in Figure 10. The new perturbation is decided based on previous and current output power as follows: if  $\Delta P \times \Delta V > 0$ , the operating voltage should increase; while if  $\Delta P \times \Delta V < 0$ , the operating voltage should decrease. The operating voltage change is accomplished by adjusting the step size  $\Delta D$  of the duty cycle  $D$  for the DC-DC converter. (The DC-DC converter will be introduced in the next section). This model has two parameters, the step size  $\Delta D$  and the time between iterations. The smaller the P&O step size, the more accurate the result however, this will result in a longer simulation time.

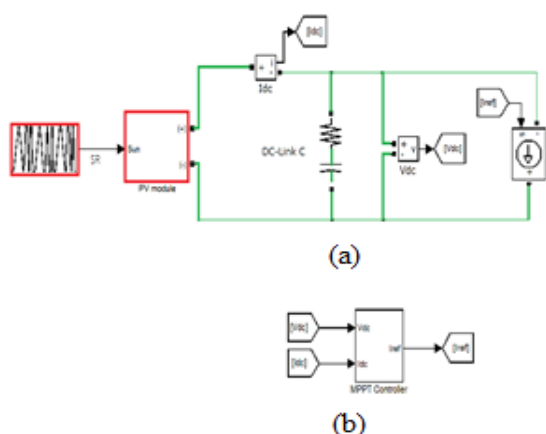


Figure 9: Control circuit used for simulation

The parameters of the system studied in this paper are summarized in Table 2.

Table 2: System Parameters

Solar panel characteristics at STC	
Open-circuit voltage	900 V
Voltage at MPP	700.2 V
Short-circuit current	20 A
Current at MPP	17.6 A
DC-Link Capacitor	
Capacitance	700 $\mu$ F
ESR	1 m $\Omega$
Sampling frequency	
MPPT algorithm	25 Hz
V and I measurements	20 kHz

The characteristics of the solar array were chosen in order to fulfill the requirements of the inverter. The input voltage of the inverter ( $V_{MPP}$ ) has to be greater than the peak line-to-line voltage of the output ( $\sqrt{6} \times 230 \text{ V} \approx 563 \text{ V}$ ). The current was selected so that the power level is over 100 MW. The sample frequency of the MPPT algorithm should not be very high because the changes in the weather conditions are relatively slow compared to the dynamics of systems typically studied in control theory, whereas the sampling frequency of the voltage and current measurements was chosen according to the sampling time of a modern DSP.

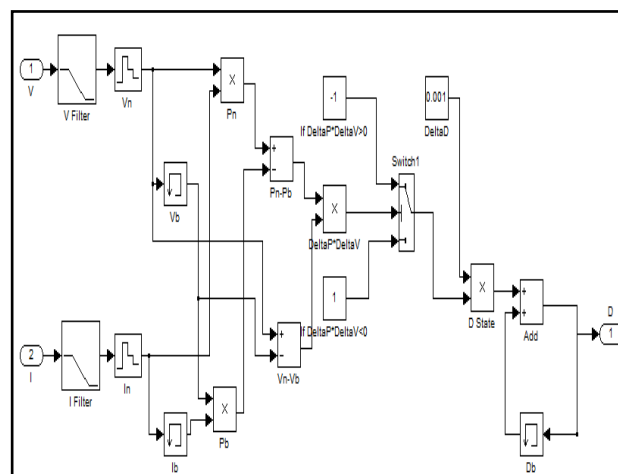


Figure 10: Simulation model for P&O MPPT algorithm

### 3) DC-DC Converter with PV Module Simulation

The output voltage of a PV system is very low and fluctuates, as the SR and temperature change daily and seasonally. Therefore, a DC-DC converter is used to get constant high output DC voltage. Furthermore, a DC-DC converter serves the purpose of transferring maximum power from the solar PV cell to the load. The converter acts as an interface between the load and the PV cell. By changing the duty cycle  $D$ , the load impedance is varied and

matched at the point of the peak power with the source, so as to transfer the maximum power [10]. There are four basic configurations and topologies of DC-DC converters as buck, boost, buck-boost and cuk. The boost type converter is considered the most advantageous to implement together with the MPPT algorithm for the following reasons:

- The output voltage is always higher than the input PV cell voltage, which is useful as the PV cell needs to be connected to the grid eventually.
- The topology of the boost converter is simple, easy to implement, low cost and has high efficiency.
- The control of the boost converter is also relatively easy hence fluctuations can be minimized and also there is increase tracing accuracy.

The function of a boost converter is to regulate the output voltage from the PV array at different operating conditions. Figure 11 shows the topology of a DC-DC boost converter, as a combination of power semiconductor switch operating at a switching frequency, a diode and an LC filter. For this converter, power flow is controlled by means of the on/off duty cycle of the switching transistor. When the switch is 'On' for  $t_{on}$  seconds, current flows through the inductor in clockwise, and energy  $V_i I_L t_{on}$  is stored in the inductor. When the switch is 'Off' for  $t_{off}$  seconds, current will be reduced for increasing impedance. The only path of the inductor current is through diode D to the capacitor C and resistive load R. The polarity of the inductor will change. The energy accumulated in the inductor during the On-state will be released,  $(V_c - V_i) I_L t_{off}$ .

Hence,

$$V_i I_L t_{on} = (V_c - V_i) I_L t_{off} \quad (1)$$

Therefore,

$$V_c = \frac{t_{off}}{t_{on} + t_{off}} V_i = \frac{T}{t_{off}} V_i = \frac{1}{1+D} V_i \quad (2)$$

where  $D$  is the duty cycle, which is the fraction of the commutation period  $T$  during which the switch is On. Since  $\frac{T}{t_{off}} \geq 1$ , the output voltage is always higher than the source voltage.

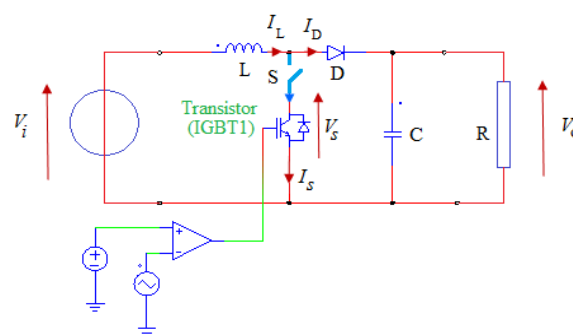


Figure 11: Topology of DC-DC boost converter

The circuit model of the DC-side of the proposed GCPV system is shown in Figure 13. It is composed of the developed circuit PV module model with a DC-DC boost converter model. A PWM boost converter of parameters shown in Table 3 is used for MPPT. The simulation model for the DC-DC converter is shown in Figure 12.

Table 3: Parameters of the DC-DC Converter PSIM

Parameter	Value
Inductor L	0.01 H
Capacitor C	$2 \times 10^{-3}$ F
Capacitor C <sub>1</sub>	$2 \times 10^{-3}$ F
Resistor R	500 $\Omega$

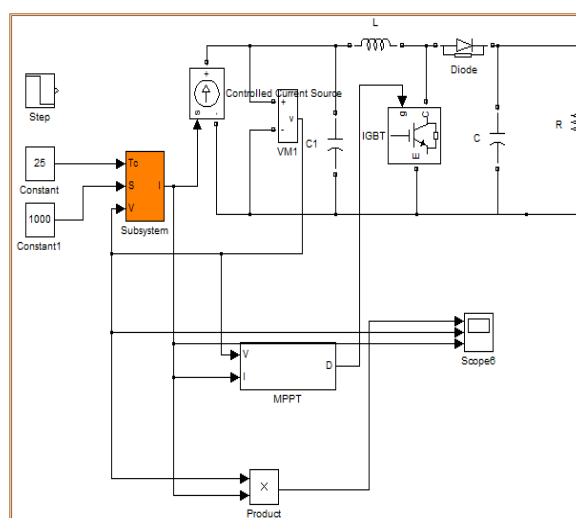


Figure 12: Simulation model for DC-DC converter

When temperature and SR are fixed,  $T = 25^\circ\text{C}$  and  $SR = 1000 \text{ W/m}^2$ , it can be seen from Figure 14 that the system reaches the maximum power point at a time  $t = 0.2$  s. The time  $t = 0$  to  $t = 0.05$  s is a period for the system to initiate its state, at time  $t = 0.05$  s the

PV cell has output voltage, but its current is zero therefore the output power is zero too. From time  $t = 0.05$  s to  $t = 0.2$  s, the simulated voltage output with the MPPT control based on P&O method overshoots and undershoots. However, after  $t = 0.2$  s, the voltage value oscillates around 36 V in a very regular manner. This is due to the P&O method used here.

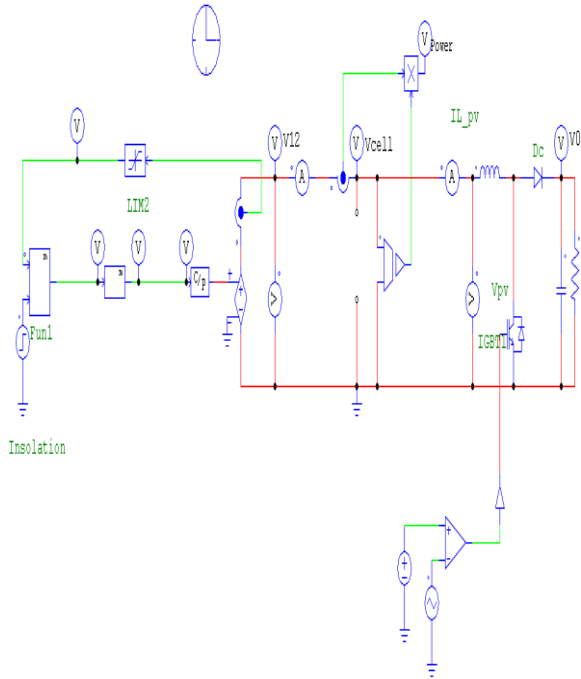


Figure 13: PV module with step up DC-DC converter circuit model

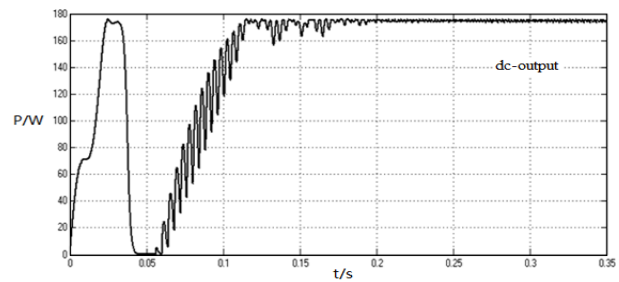
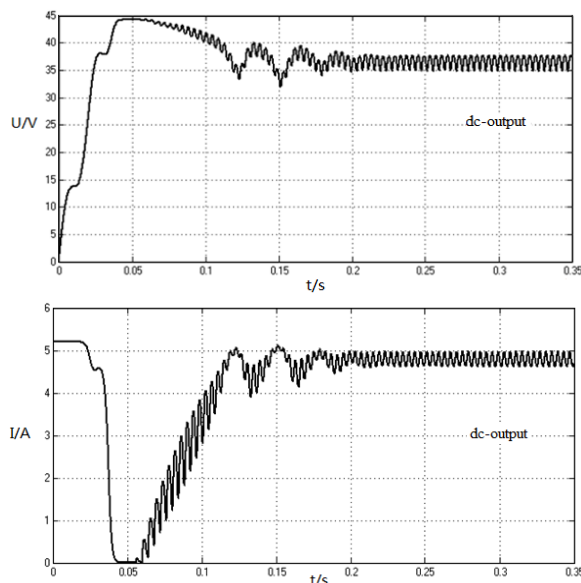


Figure 14: Simulation results for MPPT when temperature and SR keep unchanged,  $T = 25^{\circ}\text{C}$ ,  $\text{SR} = 1000 \text{ W/m}^2$

As shown in Figure 15, the boost (step-up) converter has raised the output voltage of one PV string from 2.2 kV up to 15 kV. This voltage level can be now interfaced with a suitable DC-AC inverter. The output voltage is free from ripple and it is in the real time domain. The DC output current is shown in Figure 16, ignoring the switching transient, its amplitude is 241.3 A.

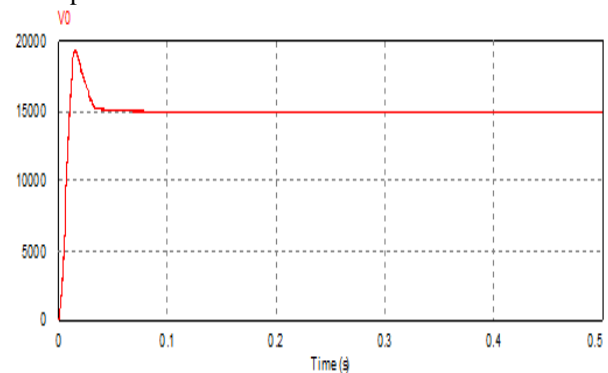


Figure 15: DC-DC boost converter output voltage of one PV string

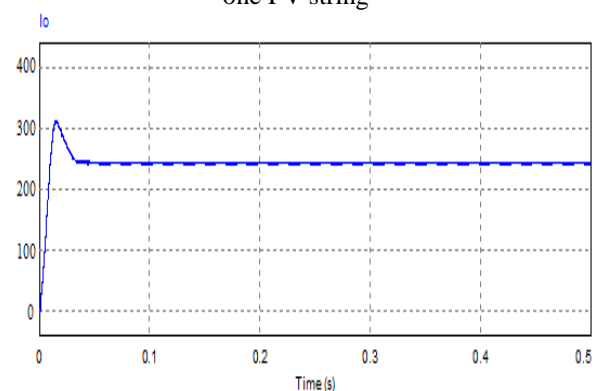


Figure 16: DC-DC boost converter output current of one PV string

In addition, the result of the DC output power of one PV panel is illustrated in Figure 17. The output power of one panel is approximately 0.710 MW and it is 94.7% of its calculated value (0.75 MW) which is very satisfactory.

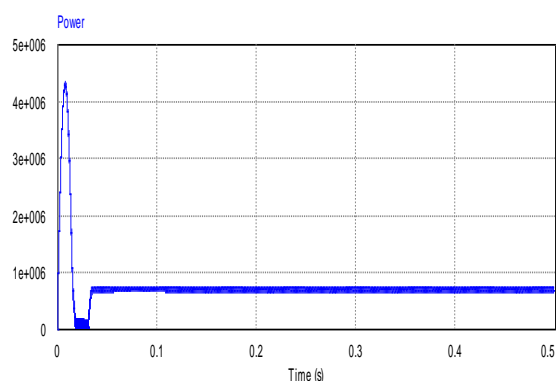


Figure 17: DC output power of one PV panel

#### 4) DC-AC Inverter Simulation Model

The DC voltage that a PV array produces has to be converted into an AC voltage so that it can be fed into Alsabyia grid. In this study a three-phase PWM inverter with a low-pass filter was employed to perform this task. The inverter is connecting the output DC bus voltage of the converter to the PV system providing the necessary conversion and regulation from the DC bus to the AC load. The output voltage is required to be sinusoidal and in phase with the grid voltage. The LC filter, which comprises an inductor and a capacitor driven by a voltage source, can generate good output voltage regulations at a particular frequency (50 Hz). Figure 18 shows the simulation model of the whole GCPV system. The inverter is controlled using a current-mode control. The reference current  $i^*$  is sent to compare with the DC-AC output current. The compared result is sent to a discrete PI controller to generate signals for a PWM generator. The PWM signal can be used to control switches of the inverter. The frequency of the PWM waveform is set to 5 kHz, which can reduce the switching noise, simplify the system design and improve the dynamic performance [9]. Some important parameters related to the simulation process for the whole GCPV system have been shown in Table 4.

Table 4: Parameters of the full GCPV System Simulation Model

The AC voltage source (grid voltage)	PI controller	LC filter
Peak amplitude 155.5 V	Instantaneous time $T = 5 \times 10^{-7}$	$L_1 = 10$ mH
Phase = 0	Proportional gain $K_p = 6$	$C = 2$ $\mu F$
Frequency = 50 Hz	Integral gain $K_i = 256$	

A Power Simulation Software (PSIM) has been implemented to simulate the proposed overall PV system.

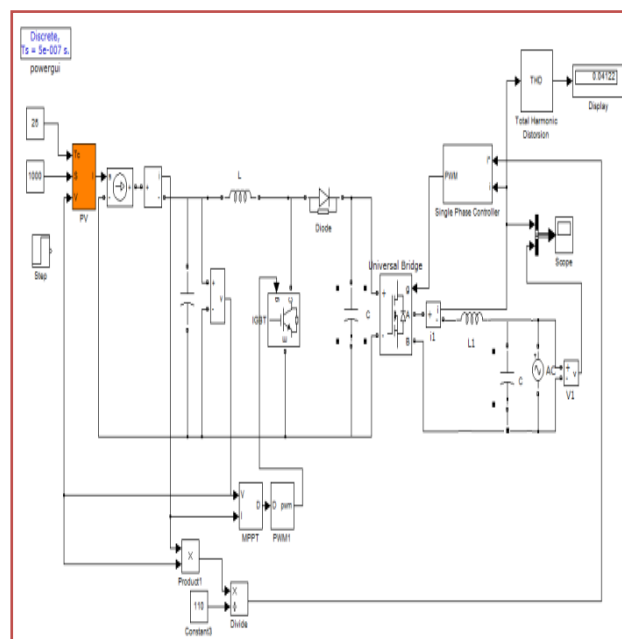


Figure 18: Simulation model of whole GCPV system

The simulation result shown in Figure 19 is obtained when the temperature and SR are kept constant at  $T = 25^\circ C$ ,  $SR = 1000 W/m^2$ . After 0.05 s, the output current of the inverter is almost sinusoidal and in phase with the grid voltage. The total harmonic distortion (THD) % of the inverter's current is 4.122%, which satisfies UL1747 standard requirements for THD [10].

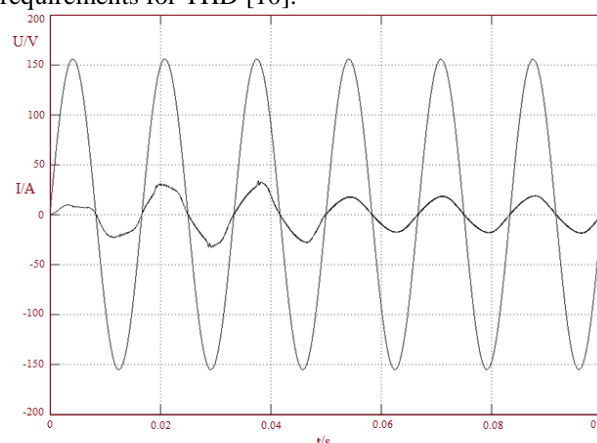


Figure 19: Simulation result when temperature and SR keep unchanged,  $T = 25^\circ C$ ,  $SR = 1000 W/m^2$

#### IV. CONCLUSIONS

In this study a full GCPV model connected to a section of Alsabyia generation station part of Kuwait national grid has been developed, simulated and analysed. The PV modules are modelled using an analytical description of PV cells. The maximum

power of the PV module is tracked with an adjusted P&O MPPT algorithm based on boost DC-DC converter. A DC-AC inverter is employed to connect the PV module to Alsabyia grid and regulate the output voltage of the converter. The effects of unchanged temperature and SR have been simulated and analysed. The whole GCPV systems was built and simulated within the PSIM package and allows easy access to all its variables and system inputs. This model provides a very good tool to design size and analyse GCPV systems in a very reasonable time and with relative high accuracy. The overall simulation model is able to maintain constant voltage and good output voltage regulations especially with an LC filter.

### REFERENCES

- [1] M. H. Kim, M. G. Simoes, and B. K. Bose, "Neural network based estimation of power electronic waveforms", IEEE Transaction on power electronics, Vol. 11, No. 2, pp. 383-389, March 1996
- [2] A. Kalirasu and S. S. Dash, "Modelling and Simulation of Closed Loop Controlled Buck Converter for Solar Installation", International Journal of Computer and Electrical Engineering, Vol. 3, No. 2, pp. 1793-8163, April 2011
- [3] J. Jervase, H. Bourdoucen, and A. Al-Lawati, "Solar Cell Parameter Extraction using Genetic Algorithms", Meas. Sci. Technol., 12, pp. 1922-1925, 2001
- [4] S. Jianhui, Y. Shijie, Z. Wei, W. Minda, S. Yuliang, and H. Huiruo, "Investigation on Engineering Analytical Model of Silicon Solar Cells", [J]. Acta Energiæ Solaris Sinica, 2001, 6(22): 439-412
- [5] M. Ahmad and S. Mekhilef, "Design and Implementation of a Multi-Level Three-Phase Inverter with Less Switches and Low Output Voltage Distortion", Journal of Power Electronics, vol. 9, pp. 594-604, 2009
- [6] S. Chin, J. Gadson, and K. Nordstrom, "Maximum Power Point Tracker", Tufts University Department of Electrical Engineering and Computer Science, 2003, pp. 1-66
- [7] J. J. Nedumgatt, K. B. Jayakrishnan, S. Umashankar, D. Vijayakumar, and D. P. Kothari, "Perturb and Observe MPPT Algorithm for Solar PV Systems-modelling and Simulation", in annual IEEE India Conference (INDICON), Dec. 2011, pp. 1-6
- [8] L. Chun-xia and L. Li-qun, "An Improved Perturbation and Observation MPPT Method of Photovoltaic Generate System", in 4th IEEE Conference on Industrial Electronics and Applications, ICIEA 2009, May. 2009, pp. 2966-2970
- [9] D. JC. MacKay, "Sustainable Energy - Without the Hot Air", UIT Cambridge, 2009. [Online] Available:<http://www.inference.phy.cam.ac.uk/sustainable/book/tex/cft.pdf>, [Accessed 21/10/2012]
- [10] UL1741, "Inverter, Converter, and Controllers for Use in Independent Power System"